

The emerald-hosting magnesite-rich rocks from Swat, NW Pakistan

MOHAMMAD ARIF & MOHAMMAD UMAR KHAN KHATTAK

Department & NCE Geology, University of Peshawar, Pakistan

ABSTRACT: *The Main Mantle Thrust melange zone in Swat contains carbonate-rich rocks (magnesite ± talc ± quartz ± chrome spinel/ Cr-magnetite/ ferritchromite ± fuchsite ± tourmaline ± chlorite) which locally host emerald mineralization. Detailed field and mineralogical studies suggest that these rocks were probably formed by talc-carbonate alteration of the spatially associated, previously serpentinized ultramafic rocks in the area. This transformation may have taken place at 250-550 °C and was probably caused by CO₂-bearing fluid released by the metamorphism of the underthrust sedimentary rocks of the Indian plate.*

INTRODUCTION

Magnesite-rich rocks - one of the diverse lithological types which lie along the Main Mantle Thrust (MMT) and, therefore, collectively known as the Main Mantle Thrust Melange Group (MMTMG) - occur as small to large bodies in the Swat area. Although magnesite itself is an important industrial mineral, the main economic significance of these rocks in the study area is that they locally (e.g. north of Mingora town and Gujar Kili village) host emerald mineralization (Fig.1). The emerald deposits of Swat are important for they have been producing one of the world's finest gemstone quality emerald for the last several decades.

Despite their important geological setting along a major suture zone and substantial economic significance for hosting emerald deposits, petrographic and mineralogical details about these magnesite-rich rocks are scarce. Such studies are important for petrogenetic as well as mineral exploration purposes and are the subject of this paper.

OCCURRENCE AND FIELD ASSOCIATION

The fine grained, relatively soft, carbonate-containing rocks of the Swat area have a greyish white to yellowish white colour locally displaying a reddish brown tint due to surface oxidation. The principal occurrences of these rocks are as follows: 1) Alpurai-Lilaunai area; 2) Barkotkai village; 3) Gujar Kili village; 4) Spin Obo-Kuh area; and 5) north of the Mingora town (Fig.1). In all these occurrences, except the Gujar Kili village, they are spatially associated with variably serpentinized ultramafic rocks. Although also occurring as small patches within the serpentinized rocks in some places, they are mostly distributed along the contact between the serpentinites and metasediments. These rocks are also traversed by abundant quartz veins that locally produce stockworks. Besides, the carbonate-containing rocks of the Mingora emerald mines area locally contain small clusters or nodules that are rich in chromite (with more than 50 modal % chromite).

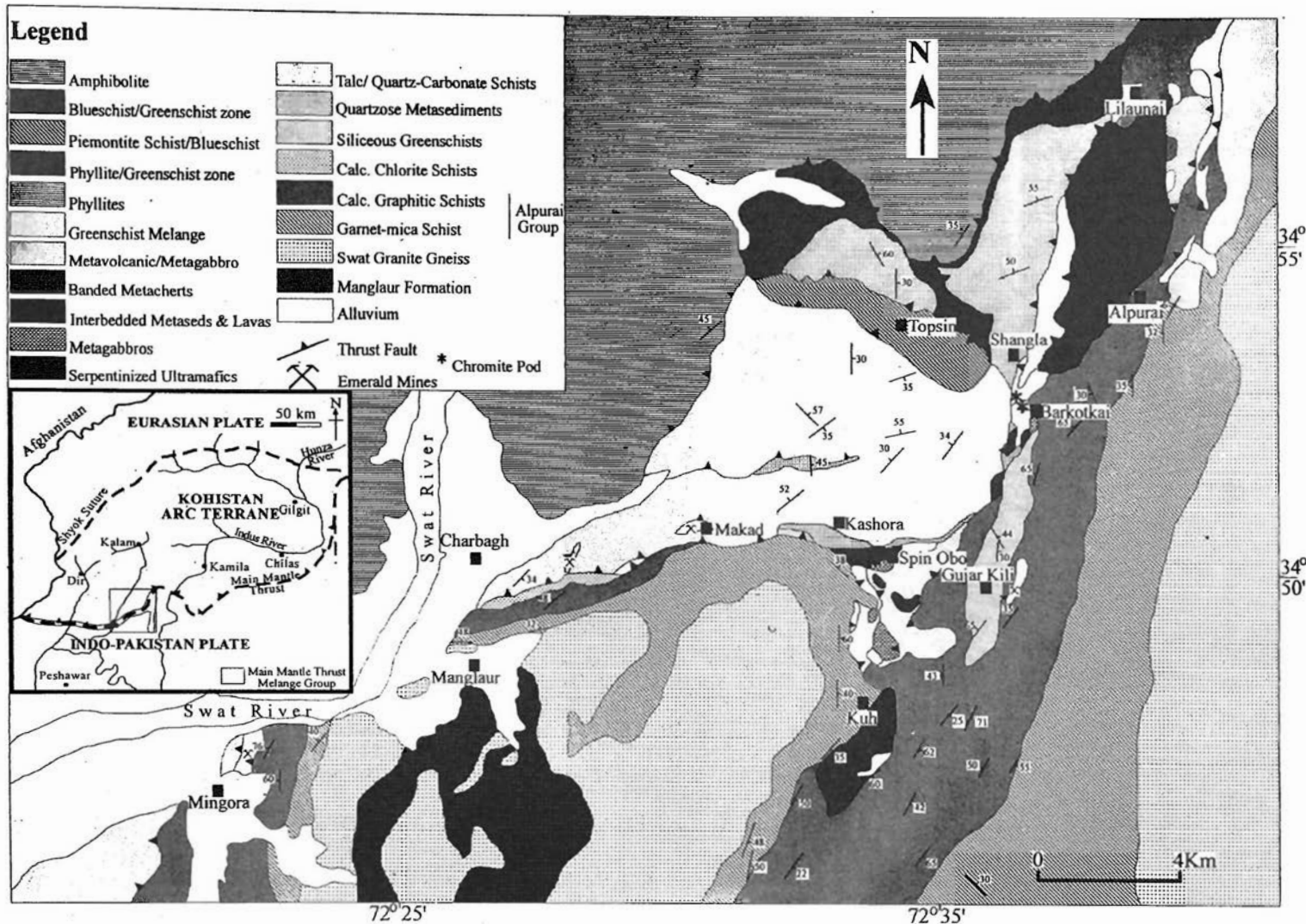


Fig. 1. Geological map of the Mingora-Lilaunai area Swat, NW Pakistan (after Hussain et al., 1982; Kazmi et al., 1984). The inset map show general location of the study area.

SAMPLES AND METHODS

A total of 139 samples representing all the different occurrences of both the carbonate-rich lithologies as well as serpentinized ultramafic rocks in the study area were collected (Fig.1). All the samples were studied petrographically and selected ones were made into polished thin sections for chemical analyses of the constituent phases.

The analyses were carried out through Jeol Superprobe model JXA-8600 with an on-line computer for ZAF corrections. Quantitative analyses were conducted using wavelength dispersive system and natural and synthetic standards under the following operating conditions: 15 Kv accelerating voltage; 30×10^{-9} A probe current; 20 (2x10) seconds peak, 10 (2x5) seconds negative background and 10 (2x5) seconds positive background counting times. The accuracy of the ZAF correction is generally better than 2%.

PETROGRAPHY

The carbonate-rich ultramafic rocks invariably consist of magnesite and accessory to trace amounts of spinel (mostly Cr-magnetite-ferritchromite and, in some cases, Cr-rich chromite) accompanied by one or more of such phases as talc, quartz and dolomite. The different relative proportion of these minerals gives rise to three principal types of assemblages: (1) talc-magnesite or magnesite-talc, depending upon whether magnesite or talc is more abundant; (2) talc-magnesite-dolomite; and (3) Quartz-magnesite. The texture of these rocks is related to the relative proportions of the different minerals, especially talc, in the paragenesis. That is, whereas the talc-free or talc-poor quartz-magnesite assemblages are massive, the talc-magnesite rocks are strongly foliated.

In addition to the phases mentioned above, some of the magnesite-rich rocks also contain fuchsite and tourmaline. In many cases, these two minerals coexist, forming veins and clusters. They also occur as fine-grained dissemination in the rocks and are, in some cases, associated with vein quartz. Fuchsite also forms borders around grains of Cr-rich chromite in both the magnesite-rich rocks and chromite-dominated small nodules. In one of the rocks, fuchsite occurs as aggregates, clusters or clots of fine grained crystals within the magnesite matrix. These possibly represent a pseudomorphic transformation from the disseminated chrome spinel grains that were present in the parent rock. Rarely, the fuchsite itself shows alteration to chlorite.

PHASE CHEMISTRY

Talc

The composition of talc was determined in 22 samples. These consist of 20 carbonate-containing including a chromitite and two carbonate-free rocks (one each of a pervasively serpentinized and sparingly serpentinized rock). The analyses of talc closely approximate to the ideal end-member composition except that they contain variable amounts of Fe (0.74-4.17 wt% FeO*), Al (reaching up to 2.26 wt% Al₂O₃), Ni (0.07-1.29 wt% NiO) and Cr (ranging from amounts below detection limit to as much as 1.52 wt% Cr₂O₃) (Table 1).

The Fe content in the studied talc is not unusual because talc in metamorphosed magnetite-poor ultramafic rocks can contain significant amounts of this component (Vance & Dungan, 1977; Evans & Guggenheim, 1988). The highest values of Al₂O₃ and Cr₂O₃ occur only in talc from the carbonate-free, sparingly serpentinized sample. Talc in this sample occurs along margins and cracks in, and hence clearly develops from, grains of

TABLE 1. REPRESENTATIVE MICROPROBE ANALYSES OF TALC

| Samp. | B17 | G1(12) | G2(6) | L24 | M1(5) | M5(5) | M6(6) | M7(5) | M13(12) | M30 | M30 | Sp43 |
|--------------------------------|--------|--------------|--------------|--------|--------------|--------------|--------------|--------------|--------------|--------|--------|--------|
| SiO ₂ | 61.52 | 61.77±0.57 | 62.03±0.30 | 60.65 | 61.73±0.30 | 61.55±0.58 | 60.15±0.78 | 61.39±1.72 | 61.35±0.44 | 61.78 | 61.22 | 62.50 |
| TiO ₂ | 0.01 | 0.01±0.01 | 0.01±0.01 | 0.01 | 0.02±0.01 | 0.01±0.01 | 0.02±0.01 | 0.01±0.01 | 0.02±0.03 | 0.03 | 0.01 | 0.00 |
| Al ₂ O ₃ | 0.02 | 0.07±0.02 | 0.46±0.15 | 0.53 | 0.12±0.08 | 0.09±0.07 | 0.03±0.01 | 0.06±0.09 | 0.27±0.17 | 0.44 | 0.24 | 0.06 |
| Cr ₂ O ₃ | 0.03 | 0.04±0.03 | 0.17±0.11 | 0.15 | 0.04±0.04 | 0.2±0.18 | 0.03±0.02 | 0.04±0.02 | 0.12±0.09 | 0.47 | 0.29 | 0.12 |
| FeO* | 2.81 | 2.63±0.10 | 2.71±0.30 | 1.39 | 3.11±0.24 | 1.78±0.17 | 1.38±0.18 | 1.79±0.31 | 2.56±0.44 | 0.80 | 0.85 | 4.17 |
| MnO | 0.01 | 0.02±0.01 | 0.02±0.01 | 0.00 | 0.01±0.02 | 0.02±0.01 | 0.02±0.01 | 0.03±0.01 | 0.02±0.01 | 0.01 | 0.02 | 0.02 |
| MgO | 28.93 | 29.26±0.31 | 29.33±0.21 | 30.14 | 29.11±0.21 | 29.08±0.70 | 29.38±0.23 | 30.31±0.65 | 28.58±0.39 | 29.70 | 29.28 | 28.18 |
| CaO | 0.03 | 0.078±0.14 | 0.02±0.02 | 0.01 | 0.01±0.00 | 0.02±0.01 | 0.02±0.01 | 0.01±0.00 | 0.01±0.02 | 0.01 | 0.01 | 0.01 |
| Na ₂ O | 0.03 | 0.02±0.02 | 0.04±0.01 | 0.15 | 0.004±0.005 | 0.17±0.12 | 0.05±0.02 | 0.10±0.08 | 0.04±0.03 | 0.07 | 0.05 | 0.02 |
| K ₂ O | 0.01 | 0.02±0.02 | 0.01±0.01 | 0.01 | 0.02±0.02 | 0.13±0.07 | 0.02±0.02 | 0.05±0.01 | 0.01±0.00 | 0.01 | 0.02 | 0.01 |
| NiO | 0.37 | 0.28±0.06 | 0.18±0.05 | 0.09 | 0.37±0.16 | 0.48±0.14 | 0.28±0.02 | 0.31±0.03 | 0.66±0.22 | 0.42 | 0.41 | 0.22 |
| Total | 93.77 | 94.20±0.79 | 94.98±0.41 | 93.13 | 94.54±0.56 | 93.52±0.83 | 91.36±1.01 | 94.10±0.98 | 93.63±0.71 | 93.74 | 92.4 | 95.31 |
| Cations per 22 (O, OH) | | | | | | | | | | | | |
| Si | 8.010 | 7.998±0.016 | 7.966±0.019 | 7.906 | 7.981±0.011 | 8.010±0.017 | 7.987±0.019 | 7.941±0.118 | 8.001±0.026 | 7.981 | 8.017 | 8.042 |
| Ti | 0.001 | 0.001±0.001 | 0.001±0.001 | 0.001 | 0.001±0.001 | 0.001±0.000 | 0.001±0.001 | 0.001±0.001 | 0.002±0.003 | 0.003 | 0.001 | 0.000 |
| Al | 0.003 | 0.011±0.004 | 0.070±0.023 | 0.082 | 0.018±0.013 | 0.014±0.010 | 0.004±0.002 | 0.009±0.014 | 0.041±0.026 | 0.067 | 0.037 | 0.009 |
| Cr | 0.003 | 0.004±0.003 | 0.017±0.011 | 0.016 | 0.003±0.004 | 0.021±0.019 | 0.003±0.002 | 0.004±0.003 | 0.012±0.009 | 0.048 | 0.030 | 0.012 |
| Fe ²⁺ | 0.306 | 0.285±0.011 | 0.291±0.032 | 0.151 | 0.337±0.026 | 0.194±0.021 | 0.153±0.019 | 0.194±0.035 | 0.279±0.047 | 0.086 | 0.094 | 0.449 |
| Mn | 0.001 | 0.002±0.001 | 0.003±0.002 | 0.000 | 0.001±0.002 | 0.002±0.002 | 0.002±0.001 | 0.003±0.001 | 0.002±0.001 | 0.001 | 0.002 | 0.002 |
| Mg | 5.615 | 5.647±0.020 | 5.614±0.038 | 5.858 | 5.611±0.044 | 5.642±0.080 | 5.817±0.024 | 5.848±0.188 | 5.555±0.061 | 5.719 | 5.715 | 5.406 |
| Ca | 0.005 | 0.011±0.019 | 0.003±0.003 | 0.002 | 0.005±0.006 | 0.002±0.002 | 0.002±0.002 | 0.002±0.001 | 0.002±0.002 | 0.002 | 0.002 | 0.002 |
| Na | 0.007 | 0.006±0.006 | 0.010±0.002 | 0.038 | 0.001±0.002 | 0.043±0.030 | 0.014±0.006 | 0.026±0.021 | 0.010±0.007 | 0.017 | 0.013 | 0.002 |
| K | 0.002 | 0.003±0.003 | 0.002±0.001 | 0.002 | 0.003±0.002 | 0.022±0.012 | 0.004±0.003 | 0.008±0.003 | 0.001±0.001 | 0.002 | 0.004 | 0.001 |
| Ni | 0.039 | 0.029±0.006 | 0.019±0.005 | 0.009 | 0.047±0.007 | 0.050±0.015 | 0.030±0.002 | 0.032±0.003 | 0.070±0.023 | 0.044 | 0.043 | 0.023 |
| Total | 13.990 | 13.998±0.019 | 13.996±0.008 | 14.064 | 14.008±0.014 | 14.002±0.005 | 14.016±0.023 | 14.068±0.110 | 13.976±0.021 | 13.969 | 13.957 | 13.947 |

Samples designated as B, G, L and M represent the occurrences of magnesite-rich rocks in the Barkotkai, Gujar Kili, Lilaunai and Mingora areas, respectively (Fig. 1)

Numbers in parentheses refer to the total number of analyses whose mean compositions are listed

* Total iron as FeO

enstatite. The Cr_2O_3 , and perhaps also Al_2O_3 , may have been derived from the associated chrome spinel grains through alteration of the latter to ferritchromite. Another important feature of the studied talc is the variable, but in many cases high, concentration of NiO. It is probably due to the fact that talc tends to fractionate Ni with respect to other phases including even olivine (Trommsdorff & Evans, 1974).

Magnesite

Microprobe analyses of magnesite were performed in 24 samples representing all the five localities where carbonate-rich ultramafic rocks occur (Fig. 1). The grains of magnesite were analysed for FeO^* , MnO , MgO , CaO , and, in many but not all cases, for SrO . In addition, the NiO content of magnesite was also determined in some of the samples. The overall ranges (wt%) of these components are: 0.66-15.91 FeO; <0.05-2.11 MnO; 35.45-46.30 MgO; 0.02-0.91 CaO; <0.02-0.08 SrO; and 0.04-0.43 NiO (Table 2). Hence the studied magnesites range in composition from virtually Fe-free to ferroan types. The greater variability in the FeO content is partly due to the alteration of some of the magnesite grains along their outermost margins. These rather thin marginal portions have invariably high reflectance due to an increase in the sideritic component relative to the main bulk of the grains.

DISCUSSION AND CONCLUSIONS

Several lines of evidence suggest that the investigated magnesite-rich lithologies formed by alteration of ultramafic rocks rather than by a simple isochemical metamorphism of siliceous dolomite. These include (1) presence of relict pods of serpentinized ultramafic rocks within the magnesite-rich bodies, e.g. in Mingora emerald mines area (Fig. 1); (2) magnesite-

rich patches occurring along shear zones within the bodies of ultramafic rocks (Kazmi et al., 1986); (3) magnesite-rich veins cutting through felted masses of serpentinite and talc (Kazmi et al., 1989); (4) coarser grain size; (5) simple mineralogical composition, mostly consisting of two to four phases; (6) occurrence of significant Ni and Cr in talc and magnesite (Tables 1, 2); (7) presence of relict high-Cr chromite grains and segregations (Arif & Moon, 1996); and (8) except for abnormally low SiO_2 in some of them, their whole-rock chemical characteristics are broadly similar to those of typical ultramafic rocks (Arif & Moon, 1998).

Hence it appears that the magnesite-dominated lithologies have been derived from ultramafic rocks by alteration involving mainly the replacement of variable amounts of SiO_2 by CO_2 ($2\text{CO}_3^{2-} = \text{SiO}_4^{4-}$). As veins of magnesite cut across the serpentine matrix in some of the ultramafic rocks, the carbonate alteration clearly commenced after serpentinization and was probably caused by the CO_2 released during the metamorphism of metasedimentary rocks of the underlying Indian plate (Arif, 1994; Arif & Moon, 1996; Arif et al., 1996).

Keeping aside the relatively rare dolomite-bearing rocks (discussed separately below), the carbonate-dominated assemblages of the Swat valley can be grouped into two: (1) magnesite + talc \pm quartz and (2) magnesite + quartz \pm talc. In other words, the overall mineralogy of these rocks can best be expressed in terms of the four component system, $\text{MgO-SiO}_2\text{-H}_2\text{O-CO}_2$. Detailed experimental and petrological investigations of such a system have been performed by many workers (e.g. Fyfe, 1962; Greenwood, 1967; Johannes, 1969; Evans & Trommsdorff, 1974; Hemley et al., 1977).

TABLE 2. REPRESENTATIVE MICROPROBE ANALYSES OF MAGNESITE

| Samp. | B17 | B46 | G1 [†] | G1 [†] | G2 | G2 | G3 | G5 | G10 | G15 | G15 | L4 | L7 | L22 | M1 |
|-------|-------|-------|-----------------|-----------------|-------|-------|-------|-------|-------|------|-------|-------|-------|-------|-------|
| FeO* | 4.56 | 7.46 | 1.18 | 9.5 | 3.41 | 3.11 | 5.82 | 10.44 | 15.91 | 7.1 | 6.85 | 8.77 | 1.71 | 1.45 | 9.33 |
| MnO | 0.03 | 0.05 | 1.74 | 0.0 | 0.05 | 0.04 | 0.07 | 0.24 | 0.47 | 0.0 | 0.08 | 0.03 | 0.99 | 0.79 | 0.15 |
| MgO | 40.78 | 40.46 | 44.77 | 39.9 | 40.86 | 41.23 | 41.32 | 38.88 | 35.96 | 40.0 | 39.74 | 38.96 | 41.51 | 40.75 | 39.04 |
| CaO | 0.30 | 0.09 | 0.03 | 0.1 | 0.89 | 0.55 | 0.05 | 0.14 | 0.02 | 0.1 | 0.18 | 0.14 | 0.21 | 0.16 | 0.19 |
| NiO | 0.06 | 0.16 | n.a. | n.a. | 0.18 | 0.26 | 0.27 | 0.14 | 0.04 | 0.0 | 0.08 | 0.31 | 0.03 | 0.02 | 0.06 |
| Total | 45.73 | 48.22 | 47.77 | 49. | 45.39 | 45.19 | 47.53 | 49.84 | 52.40 | 47.4 | 46.93 | 48.21 | 44.45 | 43.17 | 48.77 |

Cations per three oxygens

| | | | | | | | | | | | | | | | |
|------------------|-------|-------|-------|-------|-------|-------|-------|-------|-------|-------|-------|-------|-------|-------|-------|
| Fe ²⁺ | 0.054 | 0.090 | 0.014 | 0.117 | 0.04 | 0.036 | 0.07 | 0.128 | 0.202 | 0.085 | 0.082 | 0.106 | 0.020 | 0.017 | 0.113 |
| Mn | 0.000 | 0.001 | 0.021 | 0.000 | 0.001 | 0.000 | 0.001 | 0.003 | 0.006 | 0.001 | 0.001 | 0.000 | 0.012 | 0.009 | 0.002 |
| Mg | 0.855 | 0.869 | 0.945 | 0.871 | 0.854 | 0.859 | 0.880 | 0.852 | 0.815 | 0.855 | 0.845 | 0.841 | 0.859 | 0.836 | 0.846 |
| Ca | 0.005 | 0.001 | 0.000 | 0.002 | 0.013 | 0.008 | 0.001 | 0.002 | 0.000 | 0.002 | 0.003 | 0.002 | 0.003 | 0.002 | 0.003 |
| Ni | 0.001 | 0.002 | ----- | ----- | 0.002 | 0.003 | 0.003 | 0.002 | 0.000 | 0.001 | 0.001 | 0.004 | 0.000 | 0.000 | 0.001 |
| Total | 0.915 | 0.963 | 0.980 | 0.990 | 0.910 | 0.906 | 0.955 | 0.987 | 1.023 | 0.944 | 0.932 | 0.953 | 0.894 | 0.864 | 0.965 |

| Samp. | M2 | M | M3 | M3 | M4 | M5 | M6 | M | M9 | M9 [†] | M13 | M13 | M21 | M2 | M24 |
|-------|-------|------|-------|-------|-------|-------|-------|------|-------|-----------------|-------|-------|-------|------|-------|
| FeO* | 6.36 | 6.7 | 5.24 | 7.27 | 6.89 | 8.69 | 5.87 | 13.1 | 2.04 | 15.24 | 9.85 | 7.62 | 7.56 | 6.4 | 6.23 |
| MnO | 0.15 | 0.1 | 0.16 | 0.21 | 0.07 | 0.12 | 0.36 | 0.1 | 0.03 | 0.23 | 0.19 | 0.11 | 0.07 | 0.0 | 0.06 |
| MgO | 40.22 | 40.1 | 39.97 | 39.09 | 39.98 | 39.83 | 39.15 | 39.4 | 41.61 | 35.45 | 38.17 | 38.9 | 39.17 | 39. | 40.39 |
| CaO | 0.13 | 0.0 | 0.32 | 0.18 | 0.52 | 0.14 | 0.14 | 0.0 | 0.03 | 0.27 | 0.17 | 0.1 | 0.11 | 0.0 | 0.16 |
| NiO | 0.05 | 0.0 | 0.05 | 0.10 | 0.05 | 0.06 | 0.02 | 0.2 | 0.43 | n. a. | 0.10 | 0.11 | 0.10 | 0.0 | 0.00 |
| Total | 46.91 | 47.2 | 45.74 | 46.85 | 47.51 | 48.84 | 45.54 | 53.0 | 44.14 | 51.22 | 48.48 | 46.84 | 47.01 | 46.4 | 46.84 |

Cations per three oxygens

| | | | | | | | | | | | | | | | |
|------------------|-------|-------|-------|-------|-------|-------|-------|-------|-------|-------|-------|-------|-------|-------|-------|
| Fe ²⁺ | 0.076 | 0.08 | 0.062 | 0.087 | 0.083 | 0.106 | 0.069 | 0.166 | 0.024 | 0.192 | 0.120 | 0.091 | 0.090 | 0.076 | 0.074 |
| Mn | 0.002 | 0.002 | 0.002 | 0.003 | 0.001 | 0.001 | 0.004 | 0.001 | 0.000 | 0.003 | 0.002 | 0.001 | 0.001 | 0.001 | 0.001 |
| Mg | 0.854 | 0.856 | 0.841 | 0.833 | 0.854 | 0.862 | 0.824 | 0.888 | 0.859 | 0.795 | 0.828 | 0.829 | 0.835 | 0.843 | 0.857 |
| Ca | 0.002 | 0.001 | 0.005 | 0.003 | 0.008 | 0.002 | 0.002 | 0.001 | 0.000 | 0.004 | 0.003 | 0.002 | 0.002 | 0.001 | 0.002 |
| Ni | 0.001 | 0.001 | 0.001 | 0.001 | 0.001 | 0.001 | 0.000 | 0.003 | 0.005 | ----- | 0.001 | 0.001 | 0.001 | 0.001 | 0.000 |
| Total | 0.935 | 0.940 | 0.911 | 0.927 | 0.947 | 0.972 | 0.899 | 1.059 | 0.888 | 0.994 | 0.954 | 0.924 | 0.929 | 0.922 | 0.934 |

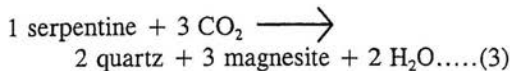
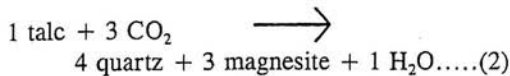
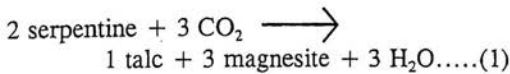
Samples designated as B, G, L and M represent the occurrences of magnesite-rich rocks in the Barkotkai, Gujar Kili, Lilaunai and Mingora areas, respectively (Fig. 1).

* Total iron as FeO

† Analysed with a carbonate program containing FeO*, MnO, MgO, CaO and SrO. The rest of the analyses were performed using a silicate program consisting of all the common major and minor oxides (i.e. SiO₂, TiO₂, Al₂O₃, FeO*, MnO, MgO, CaO, Na₂O, K₂O and NiO) and an X-ray beam diameter of 5 mm.

n. a. = not analysed

Applying the results of these studies, the following reactions would lead to the formation of the magnesite-containing rocks of the study area:



Depending upon the composition of the fluid phase and total pressure, the equilibrium temperatures for these reactions vary between 300°C and 550°C (Greenwood, 1967; Johannes, 1969; Evans & Trommsdorff, 1974). According to Johannes (1969), at a fluid pressure of 2 kb, the assemblage talc + magnesite is stable between about 350°C and 550°C and at 7 kb about 490°C and 660°C. The results of recent studies (e.g. Schandl & Naldrett, 1992; Schandl & Wicks, 1993), however, show that the talc-carbonate and quartz-carbonate assemblages may also originate at slightly lower temperatures (250-300°C). It follows, therefore, that the magnesite-rich assemblages of the investigated area might have formed in the temperature range of 250-550°C.

The rarer dolomite-bearing magnesite-talc assemblage probably represents an originally clinopyroxene (diopside)-rich ultramafic rock. The earlier episode of hydration-dominated alteration (and low grade, i.e. greenschist facies, metamorphism) of such a rock would produce a tremolite-rich schist rather than serpentinite. A further alteration of this rock by CO₂-bearing fluid is likely to yield (by converting tremolite to dolomite) a dolomite-containing assemblage.

Acknowledgements: The studies were financed by the Association of Commonwealth

Universities in UK. An earlier draft of the manuscript was read by M. J. LeBas (University of Leicester, UK), A. D. Saunders (University of Leicester, UK), and David Vaughan (University of Manchester, UK). Mr. Colin Cunningham and Mr. Rob Wilson (Department of Geology, Leicester University, UK) helped in preparing polished thin sections and performing probe analyses, respectively.

REFERENCES

- Arif, M., 1994. Studies of ultramafic rocks from Swat, northwestern Pakista: Implications for the genesis of emerald and nickeliforous phases. Unpubl. Ph. D. Thesis, University of Leicester, UK.
- Arif, M. & Moon, C. J., 1996. Chemical characteristics of chrome spinel in the magnesite-rich rocks from Swat, northwestern Pakistan. *Geol. Bull. Univ. Peshawar*, 29, 9-15.
- Arif, M. & Moon, C. J., 1998. Parentage and evolution of magnesite-rich rocks from the Indus suture zone in Swat, NW Pakistan. Proceedings of the 13th Himalaya-Karakoram-Tibet International Workshop, Peshawar, Pakistan, 20-22 April, 1998. *Geol. Bull. Univ. Peshawar*, 31, 17-19.
- Arif, M., Fallick, A. E. & Moon, C. J., 1996. The genesis of emeralds and their host rocks from Swat, northwestern Pakistan: A stable-isotope investigation. *Mineral. Dep.*, 31, 255-268.
- Evans, B. W. & Guggenheim, S., 1988. Talc, pyrophyllite, and related minerals. *Reviews in Mineralogy, Mineral. Soc. Amer.*, 19, 255-294.
- Evans, B. W. & Trommsdorff, V., 1974. Stability of enstatite + talc, and CO₂-metasomatism of metaperidotite, Val d'Efra, Lepontine Alps. *Amer. Jour. Sci.*, 274, 274-296.
- Fyfe, W. S., 1962. On the relative stability of talc, anthophyllite, and enstatite. *Amer. Jour. Sci.*, 260, 460-466.
- Greenwood, D. H., 1967. Mineral equilibria in the system SiO₂-MgO-H₂O-CO₂. In: *Researches in Geochemistry* (P. H. Abelson, ed.). John Wiley and Sons, New York, 542-567.
- Hemley, J. J., Montoya, J. W., Shaw, D. R. & Luce, R. W., 1977. Mineral equilibria in the

- MgO-SiO₂-H₂O system. II: Talc-antigorite-forsterite-anthophyllite-enstatite stability relations and some geological applications in the system. *Amer. Jour. Sci.*, 277, 353-383.
- Hussain, S. S., Dawood, H., Khan, T. & Khan, I., 1982. Geological map of the Mingora-Lilaunai area, Swat, NW Pakistan. Unpubl. Rep., Gemstone Corporation of Pakistan, Peshawar.
- Johannes, W., 1969. An experimental investigation of the system SiO₂-MgO-H₂O-CO₂. *Amer. Jour. Sci.*, 267, 1083-1104.
- Kazmi, A. H., Lawrence, R. D., Dawood, H., Snee, L. W., & Hussain, S. S., 1984. Geology of the Indus suture zone in the Mingora-Shangla area of Swat. *Geol. Bull. Univ. Peshawar*, 17, 127-144.
- Kazmi, A. H., Lawrence, R. D., Anwar, J., Snee, L. W. & Hussain, S. S., 1986. Mingora emerald deposits (Pakistan): Suture associated mineralization. *Econ. Geol.*, 81, 2022-2028.
- Kazmi, A. H., Anwar, J., Hussain, S., Khan, T. & Dawood, H., 1989. Emerald deposits of Pakistan. In: *Emeralds of Pakistan* (A. H. Kazmi & L. W. Snee, eds.). Van Nostrand Reinhold, New York, 39-74.
- Schandl, E. S. & Naldrett, A. J., 1992. CO₂ metasomatism of serpentinites, south of Timmins, Ontario. *Canad. Mineral.*, 30, 93-108.
- Schandl, E. S. & Wicks, F. J., 1993. Carbonate and associated alteration of ultramafic and rhyolitic rocks at the Hemingway Property, Kidd Creek volcanic complex, Timmins, Ontario. *Econ. Geol.*, 88, 1615-1635.
- Trommsdorff, V. & Evans, B. W., 1974. Alpine metamorphism of peridotitic rocks. *Schweiz. Mineral. Petrogr. Mitt.*, 54, 333-352.
- Vance, J. A. & Dungan, M. A., 1977. Formation of peridotites by deserpentinization in the Darrington and Sultan areas, Cascade Mountains, Washington. *Bull. Geol. Soc. Amer.*, 88, 1497-1508.